Structural Formation of Poly(ethylene terephthalate) during the Induction Period of Crystallization. 3. Evolution of Density Fluctuations to Lamellar Crystal

M. Imai*

Institute for Solid State Physics, University of Tokyo, Tokai-mura, Naka-gun, Ibaraki-ken, 319-11 Japan

K. Kaji and T. Kanaya

Institute for Chemical Research, Kyoto University, Uji, Kyoto-fu, 611 Japan

Received April 13, 1994; Revised Manuscript Received July 29, 1994®

ABSTRACT: On the basis of a new finding reported in previous studies that the structural formation in the induction period of crystallization involves a kind of phase separation of spinodal decomposition due to the orientation fluctuations of polymer segments, we have investigated the structural change of poly(ethylene terephthalate) (PET) from a structure size point of view using a small angle X-ray scattering (SAXS) technique when it was crystallized at 80 or 5 °C above the glass transition temperature, T_g, from a melt-quenched glass. A spatial density correlation analysis of the SAXS intensities reveals that the size of the dense domains caused by the density fluctuations in the induction period is fairly large compared with the lamellar thickness after crystallization, indicating that these dense domains are not the embryos predicted by the classical nucleation theory. Thus, the crystal nuclei are not formed until the dense domains grow to a certain critical size, 85 Å in this case. The critical size of crystal nuclei appearing in the dense domains just after the induction period is also determined to be 14 Å.

Introduction

According to the crystal nucleation theory,[1] nucleation is initiated by large-amplitude, localized fluctuations of some order parameter such as density, leading to the appearance of small dense regions. When these regions are larger than some critical size, they will grow and eventually crystallize. The transient time to the steady state of nucleation is called the induction time. In previous papers[2,3] we have investigated the structural formation processes of poly(ethylene terephthalate) (PET) during the induction period of crystallization using a small-angle X-ray scattering (SAXS) technique and found the following results. The scattering maximum suggesting that the formation of ordered domains appeared in the initial stage of the induction period before crystallization, and this ordering process could be divided into two stages. The ordering process in the early stage conformed fairly well to Cahn's linearlized theory,[4] and that in the late stage could be described in terms of Furukawa's scaling theory.[5] Further, it was confirmed that the cause for such phase separation is due to the orientation fluctuations of the rodlike segments of PET molecules.[6] However, the relationship between the density fluctuations in the induction period and the crystal nucleation in the crystallization stage has not been so far clarified. The purpose of this paper is to investigate the evolution of the initial density fluctuations to the lamellar crystals from a structure size point of view. These structure sizes were obtained from SAXS profiles; those for the induction period were analyzed on the basis of the spatial density correlation function for an isotropic system[7] and those for the crystallization stage were analyzed using a one-dimensional electron density correlation function[8] assuming the structure of stacking lamellar crystals. From these results we discuss the ordering process of PET when crystallized near the glass transition temperature.

® Abstract published in *Advance ACS Abstracts,* October 15, 1994.

Experimental Section

PET having a number-average molecular weight, M_n, of 25 000 and a polydispersity $M_w/M_n = 2.5$ was used for this study. This sample was purified to reduce the excess scattering from impurities; it contains only 30 ppm phosphor and 30 ppm germanium as additives. The glass transition temperature and the melting temperature of the sample are 75 and 250 °C, respectively. Then the PET pellets were melted at 290 °C for 2 min and immediately thereafter quenched in ice–water. The density of the melt-quenched sample was 1.333 g/cm^3, which agrees with the value reported for the amorphous PET,[9] and no crystalline diffraction peaks were observed in the wide-angle X-ray scattering profiles for this sample.[2] The SAXS measurement were performed at the High-Intensity X-ray Laboratory of Kyoto University.[10] The essential features of this SAXS camera are the fine-focus rotating-anode X-ray generator equipped with RU-1000 (Rigaku Inc.) being operated at 3.5 kW, a Franks-type point focusing camera having a focal spot of 0.5 mm in diameter at the detector position, a two-dimensional position sensitive detector, and an evacuated X-ray flight path to reduce the background scattering. The in-situ time-resolved SAXS measurements were performed for annealing process at 80 °C in a SAXS temperature-controlled cell. The temperature of the sample cell was raised from room temperature at a heating rate of 20 °C/min and kept at 80 °C within an accuracy of ±0.3 °C after it reached this temperature. The time-resolved SAXS patterns during the isothermal annealing process at 80 °C were observed; each was recorded for 5 min with an interval of about 0.5 min. For additional information on the SAXS experiments, refer to the previous paper.[3]

Data Analysis

The SAXS profiles obtained in the induction period were analyzed based on the spatial density correlation function for isotropic systems,[7] which is the average of the product of two electron density fluctuations at distance r, defined as

$$\gamma(r) = \langle \eta(r_1)\eta(r_2) \rangle / \langle \eta^2 \rangle_{av} \quad (1)$$

where $\eta(r_1)$ and $\eta(r_2)$ are the local density fluctuations from the average value at points r_1 and r_2, a distance r

0024-9297/94/2227-7103$04.50/0

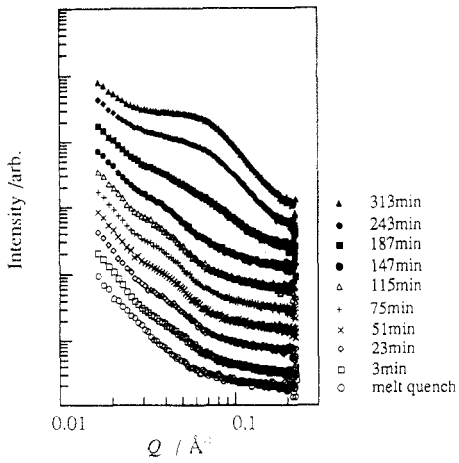

Figure 1. Time evolution of small-angle X-ray scattering (SAXS) profiles when PET was annealed at 80 °C.

apart, and $\langle\eta^2\rangle_{av}$ is the mean square of the density fluctuations. The $\gamma(r)$ function is given by the inverse Fourier transform of the scattering intensity $I(Q)$

$$\gamma(r) = \frac{\int_0^\infty I(Q)Q^2 \frac{\sin Qr}{Qr}\, dQ}{\int_0^\infty I(Q)Q^2\, dQ} \tag{2}$$

where Q denotes the magnitude of the scattering vector defined by $Q = 4\pi \sin\theta/\lambda$ with 2θ and λ being the scattering angle and the wavelength of the X-ray, respectively. To calculate the $\gamma(r)$ function for the induction period, we subtracted the intensity of the melt-quenched sample from those of the annealed samples. The difference scattering profiles show a single scattering maximum. We fit the scattering profiles using spline function and then performed inverse Fourier transformation to get the $\gamma(r)$ function.

In order to analyze the SAXS profiles for the samples in the crystallization stage, we adopted the method of one-dimensional electron density correlation function $\gamma_1(r)$ developed by Strobl et al.[8] In this model it is assumed that a partially crystalline sample consists of an ensemble of densely and isotropically packed stacks of parallel lamellae; both the normal and lateral dimensions of these stacks are large compared with the interlamellar distance. In this case, the correlation function $\gamma_1(r)$ is related to the electron density distribution along a trajectory of the normal to the lamellar surface in a stack. Thus, the $\gamma_1(r)$ function can be expressed by the scattering intensity $I(Q)$ as follows

$$\gamma_1(r) = \frac{\int_0^\infty Q^2 I(Q) \cos Qr\, dQ}{\int_0^\infty Q^2 I(Q)\, dQ} \tag{3}$$

To calculate $\gamma_1(r)$ from the observed scattering intensity using eq 3, we subtracted the intensity of the melt-quenched sample from those of the crystallized samples, taking into account of their crystallinity. After the subtraction, we fit the scattering profiles using spline functions and performed inverse Fourier transformation.

Experimental Results

According to the thermal analysis[2] of the annealing process of PET at 80 °C, the initial stage until 120 min corresponds to the induction period and then crystallization starts. Figure 1 shows the time-resolved SAXS profiles at 80 °C in double logarithmic expression. For convenience, each curve is shifted along the intensity axis. In Figure 1, the scattering profiles of the samples annealed for 3, 23, 51, 75, and 115 min correspond to the induction period, and those for 147, 187, 243, and 313 min correspond to the crystallization stage. From these scattering profiles, it is noticed that after annealing for 3 min the scattering intensity in the Q range of 0.03–0.05 Å^{-1} increases with annealing time during the induction period. After the induction period, another new scattering peak assigned to the usual long period appears near Q = 0.06 Å^{-1}, and increases in intensity with time. In order to characterize this structural formation process, we calculated the total integrated intensity I_{inv} given by

$$I_{inv} = \int_0^\infty I(Q)Q^2\, dQ \tag{4}$$

In Figure 2 we show the annealing time dependence of I_{inv}. This figure shows that the annealing process can be divided into three stages: (I) the annealing time until 30 min, where the integrated intensity increases exponentially with annealing time, (II) from 30 to 120 min, where it deviates from the initial exponential increase and levels off, and (III) from 120 to 300 min, where it rises up again with annealing time. Comparison of this profile with the results of thermal analysis reveals that the initial two stages until 120 min correspond to the induction period and the final stage corresponds to the crystallization stage.

First we consider the behavior of the density fluctuations during the induction period. Figure 3 shows the difference scattering profiles for the induction period obtained by subtracting the intensity of the melt-quenched sample from those of the annealed samples. This figure makes clear that the single scattering maximum appears at around Q = 0.04 Å^{-1} immediately after the initiation of annealing. As the annealing time increases, the maximum position shifts toward smaller Q simultaneously with increase of the maximum intensity.

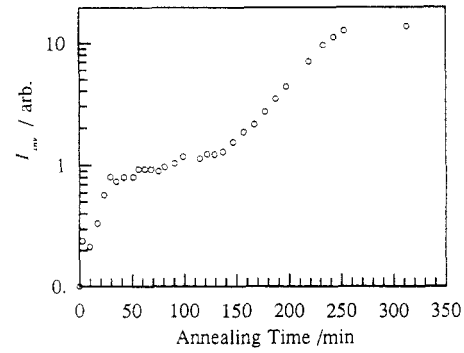

Figure 2. Annealing time dependence of total integrated SAXS intensity.

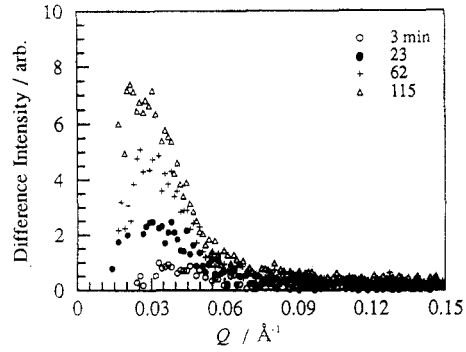

Figure 3. Difference SAXS intensity profiles for the induction period after subtraction of that of the melt-quenched sample.

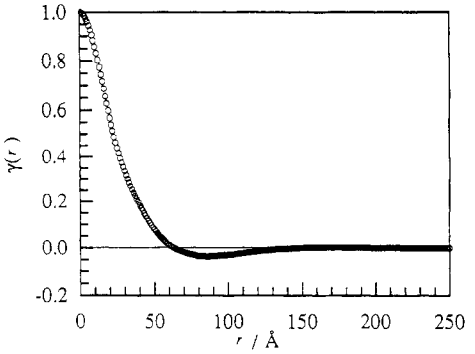

Figure 4. $\gamma(r)$ function calculated from SAXS profile for the 3 min annealed sample at 80 °C.

In stage I, the scattering maximum position at $Q = 0.04$ Å^{-1} does not move with annealing time. This scattering behavior conforms to Cahn's linearlized theory[4] predicting that the wavelength of density fluctuations keeps a constant value and the amplitude of the fluctuations increases exponentially with annealing time. Here we analyzed the scattering profiles using the spatial density correlation function $\gamma(r)$. Figure 4 shows the calculated $\gamma(r)$ function for 3 min annealed sample. The mean dense domain size is given by the value of the r axis intercept to be 62 Å.

In stage II, the scattering maximum position shifts toward smaller Q with increase of the maximum intensity. This behavior agrees with Furukawa's scaling theory[5] predicting that the amplitude of the density fluctuations grows with annealing time while it keeps self-similarity. Then the scattering profile can be scaled by the universal structure function $\tilde{S}(x)$ given by

$$\tilde{S}(x) = \frac{3x^2}{2 + x^6} \tag{5}$$

with

$$x = Q/Q_m$$

where $\tilde{S}(x)$ was normalized as $\tilde{S}(1) = 1$ and Q_m is the wavenumber at the maximum intensity. Komura et al.[11] calculated the Fourier transform $R(y)$ of $\tilde{S}(x)$ given by

$$R(y) = \frac{1}{2\pi^2}\int_0^\infty x^2\tilde{S}(x)\frac{\sin(xy)}{xy}\,dx \tag{6}$$

with the transformation of the variable from x to $y = Q_m r$. The value of the numerical calculation gives the y axis intercept of $y_1 = 2.571$. The value y_1 is related to the mean dense domain size, D_1, by

$$D_1 = y_1 Q_m^{-1} = 2.571 Q_m^{-1} \tag{7}$$

Figure 5 shows the time dependence of the dense domain in the induction period. The initial dense domains in stage II have the diameter of about 65 Å, which agrees with the size of the dense region formed in stage I. These clusters grow with annealing time, obeying the power law $D_1(t) \sim t^a$ with $a = 0.25$ as shown in a previous paper.[1] At the final stage of the induction period, D_1 grows up to 85 Å.

Upon entering stage III from the stage II, crystallization begins with formation of critical crystal nuclei, which grow into the stacked lamellar structure to cause a long-period scattering peak. In Figure 6 we show the time evolution of the difference scattering intensity multiplied by the Lorentz factor Q^2 in stage III. Here we analyzed scattering profiles after 187 min because before this time it was very

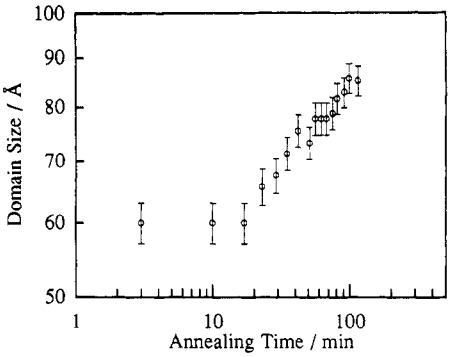

Figure 5. Annealing time dependence of the dense domain size during the induction period.

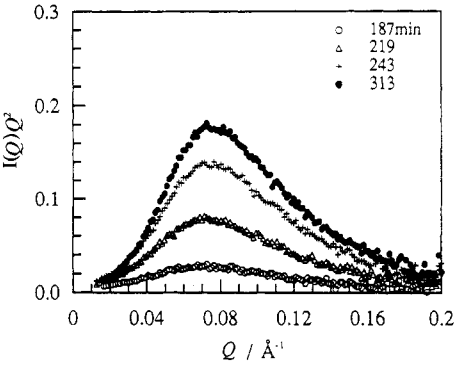

Figure 6. Annealing time evolution of difference SAXS intensity in the crystallization stage where corrections for Lorentz factor were performed.

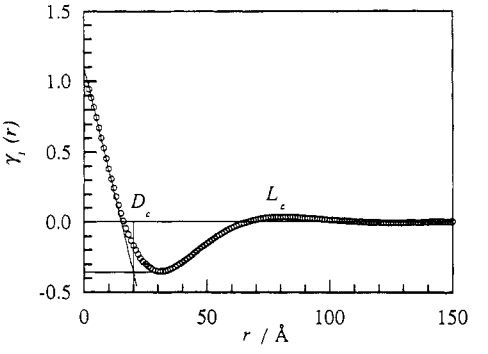

Figure 7. $\gamma_1(r)$ function calculated from difference SAXS profiles for the 219 min annealed sample.

hard to separate the scattering intensities from the density fluctuations in the induction period and lamellar crystals. A single scattering maximum caused by stacked lamellar crystals is seen in every profile; for the 187 min annealed sample it appears at around $Q = 0.07$ Å^{-1}. The maximum intensity increases with annealing time, but its position does not change. In order to estimate the characteristic size of the lamellar structure, we analyzed the obtained SAXS profiles, on the basis of the model of the one-dimensional electron density correlation function $\gamma_1(r)$.[8] Figure 7 shows $\gamma_1(r)$ for the 219 min annealed sample as an example. From this profile we can get the mean lamellar thickness, D_c, and the most probable long spacing, L_c, as shown in the figure. Remembering the Babinet's principle, we cannot however assign the D_c value thus obtained directly to the crystal thickness because it does not deny the alternative possibility that D_c is attributed to the thickness of the amorphous layer. We have therefore tried to directly estimate the crystal thickness using a wide-angle X-ray diffraction (WAXD) method. The WAXD profile for the 313 min annealed sample is shown in Figure 8 as an example. Using a curve fitting technique, we separated each diffraction peak and calculated the crys-

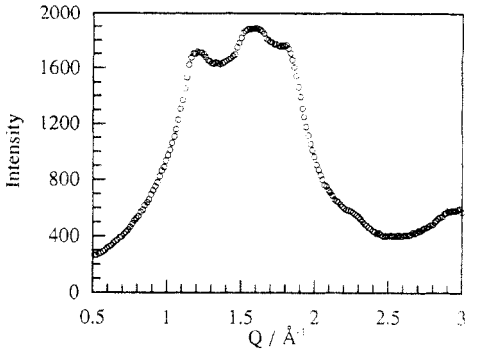

Figure 8. Wide-angle X-ray scattering profile for the 313 min annealed sample at 80 °C.

Table 1. Crystallite Size Evaluated from WAXD Peaks for the 313 min Annealed Sample

hkl	peak position (Å^{-1})	crystallite size (Å)
010	1.24	22
$\bar{1}10$	1.59	24
100	1.81	22
$0\bar{1}1$	1.16	32

tallite size by Scherrer's equation. The obtained values are in the range of 20–30 Å as shown in Table 1. In order to compare these values with the D_c value obtained from the SAXS analysis the crystallite size along the c-axis, $\bar{D}_{001}$, is required. Unfortunately there existed no possible reflections giving such crystal thickness directly. Further, the low crystallinity (about 15%) of the sample did not show a sufficient number of reflections to determine the form ellipsoid of the crystallite. The only possible method to estimate it roughly is to calculate from the crystallite size $\bar{D}_{0\bar{1}1}$ in the direction number to the inclined lattice plane $(0\bar{1}1)$ using the simple relation

$$\bar{D}_{001} = \bar{D}_{0\bar{1}1} \cos \chi_{0\bar{1}1} \tag{8}$$

where $\chi_{0\bar{1}1}$ is the angle between the $(0\bar{1}1)$ and (001) lattice planes. The value estimated from eq 8 would provide the upper limit if the long main axis of the for ellipsoid is assumed to be in the direction near the normal of the $(0\bar{1}1)$ plane. From the lattice parameters of the PET crystal system (a = 4.56 Å, b = 5.94 Å, c = 10.75 Å, α = 98.5°, β = 118°, γ = 112°), we can calculate $\chi_{0\bar{1}1}$ as 27°, so $\bar{D}_{001}$ becomes about 28 Å. This value agrees virtually with D_c = 22 Å, the value obtained from SAXS analysis. Moreover, our value of D_c is consistent with the result of the annealing temperature dependence of the lamellar thickness reported by Groeninckx et al.[12,13] Assuming the structural model for crystalline polymers in which lamellar stacks giving the regular alternation of crystalline and amorphous regions are densely packed in the sample, they estimated the mean thickness of the crystalline lamellae by combining the SAXS long period and the degree of crystallinity of the sample determined from DSC data. For a PET sample isothermally crystallized at 100 °C, they obtained a mean crystalline thickness of 26 Å from the long period of 95 Å and the degree of crysallinity of 27%. This crystalline thickness agrees nearly with our value of D_c = 22 Å for the sample crystallized at 80 °C. Although it is unknown whether or not the lamellar stack model is valid even for the sample crystallized at 100 °C, the crystalline thickness of 26 Å may be considered to be a reasonable value because the lamellar thickness obtained above changed continuously from 26 to 77 Å as the crystalline temperature T_x was increased from 100 to 245 °C and the electron micrographs of the samples crystallized at T_x > 186 °C showed the dense packing of lamellar stacks,

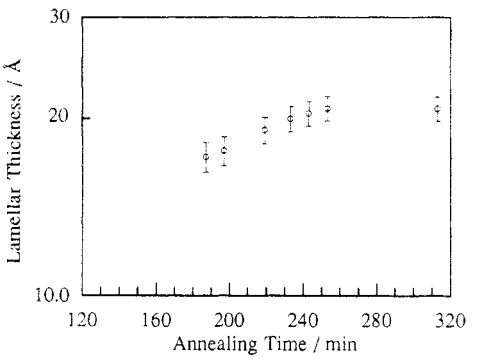

Figure 9. Annealing time dependence of the lamellar thickness.

supporting the validity of the model. Then we attributed the D_c to the mean lamellar thickness. The annealing time dependence of D_c is plotted in Figure 9. In the annealing time range of 187 to 250 min, D_c appears to increase exponentially with annealing time, and the annealing time dependence of the lamellar thickness can be expressed by

$$D_c = D_0 \exp(\alpha(t - t_0)) \tag{9}$$

where D_0 is the initial lamellar thickness, α is the thickening rate, and t_0 is the induction period. This dependence is consistent with the lamellar thickening behavior of stacked, folded chain crystals caused by annealing or isothermal crystallization,[14] and the values for D_0 and α were 14 Å and 0.0034 min^{-1}, respectively. After 250 min, the thickening rate levels off.

Discussion

Our experimental results revealed that the crystallization process is composed of the following two steps: (1) the density fluctuations appears during the induction period of crystallization, and (2) after the size of the density fluctuations grows to a certain value, crystallization begins and the stacked lamellae are formed. Considering that the growth process of the density fluctuations is a pretransitional phenomenon prior to the crystal nucleation, we try to explain the polymer nucleation within a framework of the classical nucleation theory.[15] According to this theory, the free energy for the nucleation is determined by the balance of the surface energy and the bulk energy of a crystallite. In the case of polymer crystallization, this free energy of primary nucleation, ΔF, is given by

$$\Delta F = 2\nu a\sigma_e + C\sqrt{\nu a}l\sigma_s - \nu al\Delta f \tag{10}$$

where ν is the number of segments having the cross sectional area a and thickness l, σ_e and σ_s are end and lateral surface energy, respectively, Δf is the free energy difference between the supercooled liquid and the crystal per unit volume, and C is the shape coefficient of nucleus. The thickness l^* of a critical nucleus corresponding to a saddle point in ΔF is given by

$$l^* = 4\sigma_e/\Delta f \tag{11}$$

Then the nucleation is initiated by large amplitude, localized fluctuations of density, leading to the appearance of small nuclei. If these nuclei are smaller than the critical size l^*, they will disappear, while nuclei larger than l^* will go on growing. This transient time to the steady state of nucleation is called the induction period, and nuclei smaller than the critical size are called embryos. Although it might

be considered that the density fluctuations observed in the induction period are related to the embryo, the observed size of the dense domains is much larger than the initial lamellar thickness. Thus, as is clear from Figures 5 and 8, the former is about 85 Å at the final stage of the induction period and the latter is 14 Å. This means that the dense domains in the induction period are not the embryos predicted by the classical nucleation theory. What is the nature of the density fluctuations in the induction period of crystallization? In the following we will discuss this problem.

The phenomenological kinetic equation for the first-order phase transition is given by[16]

$$\frac{\partial S}{\partial t} = -L\left(\frac{\partial A}{\partial S}\right) \tag{12}$$

$$L = L_0(-i\nabla)^{\alpha} \tag{13}$$

$$\alpha = \begin{cases} 0 \text{ for nonconserved system} \\ 2 \text{ for conserved system} \end{cases}$$

where S is the order parameter, L is phenomenological kinetic coefficient, L_0 is a constant, and A is the total free energy. In the linearlized theory, the free energy can be expressed by

$$A(S) = \int \left[\frac{1}{2}\left(\frac{\partial^2 f}{\partial S^2}\right)S^2 + \kappa(\nabla S)^2\right] dV \quad (\kappa > 0) \tag{14}$$

where $f(S)$ is the local free energy density of a homogeneous material and the second term corresponds to the free energy to create the density gradient. Let $S_Q(t)$ be the Fourier component of $S(\boldsymbol{r},t)$, then the kinetic equation becomes

$$\frac{\partial S_Q}{\partial t} = \Gamma_Q S_Q \tag{15}$$

$$\Gamma_Q = LQ^{\alpha}\left\{-\left(\frac{\partial^2 f}{\partial S^2}\right) - 2\kappa Q^2\right\} \tag{16}$$

where Γ_Q is the growth rate of the fluctuations having the wavenumber Q. For a nonconserved system ($\alpha = 0$), the Γ_Q has a maximum at $Q = 0$. Then we cannot observe the scattering maximum. On the other hand, for a conserved system ($\alpha = 2$), the fluctuations at $Q = 0$ cannot grow because of the conservation law, and for $Q \neq 0$, the growth manner of the fluctuations depends on the value of $(\partial^2 f/\partial S^2)$. When $(\partial^2 f/\partial S^2)$ is positive, i.e., in the metastable region, the fluctuations cannot grow but rather disappear. When $(\partial^2 f/\partial S^2)$ is negative, i.e., in the unstable region, the fluctuations have a maximum growth rate at $Q_m = \{(\partial^2 f/\partial S^2)/2\}^{1/2}$. Our SAXS measurements show that in the early stage of the induction period the scattering maximum appears at $Q_m = 0.04$ Å^{-1} and increases in intensity exponentially with annealing time. These behaviors of scattering profiles agree well with the prediction of the kinetics for the conserved system in the unstable region. When the frozen amorphous structure is kept just above the glass transition temperature, it is not in the metastable state but in the unstable state, so that the kinetics of structure formation in the induction period obeys the spinodal decomposition. However, is the system really conserved in the induction period of crystallization? According to the density measurement,[2] the macroscopic density of the sample doesn't change from that of the amorphous sample within experimental error (0.15%) in the induction period of crystallization, and after the induction period the density begins to increase with annealing time.

After the induction period, the stacked lamellar structure is formed and then the usual lamellar thickening occurs with time.[14] The important result is that the initial lamellar thickness can be estimated as about 14 Å. This size is fairly small compared with the size of dense domains observed in the induction period and very close to the critical size for the orientational ordering predicted by Doi et al.[17] Doi et al. developed the kinetics of orientation fluctuations of rodlike polymer which take into account (1) excluded volume effect, (2) topological effect such as entanglements, and (3) hydrodynamics, and they showed that when the system satisfies a critical condition, spinodal decomposition takes place, resulting in a phase transition from isotropic to parallel ordered nematic phase. In a previous paper,[6] we found using a depolarized light scattering technique that the parallel ordering of polymer chains actually occurs in the induction period of crystallization of PET and this ordering process obeys Doi's kinetics well. In the case of the crystallization of PET, the critical condition where the orientational ordering is observed is that in which the length of the rodlike segments exceeds 13.5 Å. Then we considered that the rodlike segments in the parallel ordered state make the initial lamellar stem.

In connection with our observations of the spinodal decomposition due to the orientation fluctuations of polymer segments during the induction period of crystallization from the *isotropic* PET glass, it may be noteworthy to refer to interesting SAXS studies by Strobl et al.[18] showing that if crystallization is conducted starting from an *oriented* PET glass, density fluctuations appear all over the sample and grow continuously in amplitude up to the final stage given by the crystalline–amorphous layer structure. They explained this phenomenon in terms of the Cahn–Hilliard theory for spinodal decomposition because the time evolution of the SAXS intensity $I(Q)$ at Q follows an exponential law. As a possible cause for this phase separation, they considered conformational defects such as entanglements, sharp folds, or chain torsions. Thus, a process of defect clustering was assumed to involve spinodal decomposition into two phases, defect-free crystalline and defect-rich amorphous regions. Although it is unknown if the Cahn–Hilliard theory is valid for the crystallization stage, because we observed the initial and late stages of spinodal decomposition before crystallization, their concept of the continuous spinodal crystallization mode is very attractive and may be considered to be an extension of our idea.

On the basis of the above discussion, we consider a structural formation model in the crystallization of PET below. When PET is annealed above the glass transition temperature from the glassy state, the frozen gauche conformations in the amorphous glassy state begin to transform to the trans conformations. This conformational change leads to the increase of the apparent rod length of the segment, which makes the parallel ordering of the segments obey the spinodal decomposition kinetics because the length of the rod segments exceeds the critical condition. The parallel ordered domains with higher density than that of the disordered region grow with annealing time. When such parallel ordered dense domains grow to a certain size, longitudinal adjustment occurs, resulting in the more efficient packing of the parallel oriented chains to form crystal nuclei. According to our experimental results, the final size of the dense domains in the induction period is 85 Å and is several

times larger than the initial lamellar thickness of 14 Å, which is very close to the critical rod length. Then it is considered that the region required to achieve the parallel packing of the chains is several times as large as the lamellar thickness to be formed because the topological effects such as entanglements obstruct the diffuse of polymer chains. Once the lamellar crystals are formed, they grow, obeying the usual lamellar thickening mechanism.

Acknowledgment. We are indebted to the Committe of the High Intensity X-ray Laboratory of Kyoto University for the small-angle X-ray scattering system. We would also like to express our sincere thanks to Dr. H. Hayashi and Dr. S. Suehiro for experimental support and helpful discussions.

References and Notes

(1) Kelton, K. F. *Solid State Physics*; Ehrenreich, H.; Turnbull, D., Ed.; Academic Press: New York; 1991, Vol. 45.
(2) Imai, M.; Mori, K.; Mizukami, T.; Kaji, K.; Kanaya, T. *Polymer* **1992**, *33*, 4451.
(3) Imai, M.; Mori, K.; Mizukami, T.; Kaji, K.; Kanaya, T. *Polymer* **1992**, *33*, 4457.
(4) Cahn, J. W. *J. Chem. Phys.* **1965**, *42*, 93.
(5) Furukawa, H. *Adv. Phys.* **1985**, *34*, 703.
(6) Imai, M.; Kaji, K.; Kanaya, T. *Phys. Rev. Lett.* **1993**, *71*, 4162.
(7) Debye, P.; Bueche, A. M. *J. Appl. Phys.* **1949**, *20*, 518.
(8) Strobl, G. R.; Schneider, M. *J. Polym. Sci. Polym. Phys. Ed.* **1980**, *18*, 1343.
(9) Fischer, E. W.; Fakirov, S. *J. Mater. Sci.* **1976**, *11*, 1041.
(10) Hayashi, H.; Hamada, F.; Suehiro, S.; Masaki, N.; Ogawa, T.; Miyaji, H. *J. Appl. Cryst.* **1988**, *21*, 330.
(11) Komura, S.; Osamura, K.; Fujii, H.; Takeda, T. *Phys. Rev. B* **1985**, *31*, 1278.
(12) Groeninckx, G.; Reynaers, H.; Berghams, H.; Smets, G. *J. Polym. Sci. Polym. Phys. Ed.* **1980**, *18*, 1311.
(13) Groeninckx, G.; Reynaers, H. *J. Polym. Sci. Polym. Phys. Ed.* **1980**, *18*, 1325.
(14) Fischer, E. W.; Schmit, G. F. *Angew. Chem.* **1962**, *74*, 551.
(15) Lauritzen, J. I.; Hoffman, J. D. *J. Appl. Phys.* **1973**, *44*, 4340.
(16) Kawasaki, K. *Busseikenkyu* **1985**, *43*, 181.
(17) Shimada, T.; Doi, M.; Okano, K. *J. Chem. Phys.* **1988**, *88*, 7181.
(18) Strobl, G. R. *Trends in Non-Crystalline Solids*; Conde, A.; Conde, C. F.; Millan, M., Eds.; World Scientific: Singapore, 1992; p 37.